ISSN: 0067-2904

Effect of Annealing Times on the Structural and Optical Properties of PbO Thin Films Prepared by D.C Sputtering

Aws Faisal Rauuf, Kadhim A. Aadim
Department of Physics, College of Science, University of Baghdad, Baghdad, Iraq.

Received: 8/6/2022 Accepted: 13/9/2022 Published: 30/6/2023

Abstract:
In this work, lead oxide (PbO) thin films were deposited using D.C. sputtering method on a surface of glass substrates and then thermally annealed at a temperature of 473K with annealing times of (1,2 and 3) hours. The structural, morphological, and optical properties of films were determined using X-ray diffraction (XRD), atomic force microscopy (AFM), FT-IR, and UV-Visible spectroscopy. The structure studies confirmed that PbO films are polycrystalline structures in an orthorhombic phase with average grain size (24.51, 29.64, 46.49, 16) nm with increasing annealing time. From AFM, the roughness of the film surface (3.26, 1.76, 1.61, 1.79) nm as the film annealing time increases. The optical band gap values of the PbO thin films are (3.9, 2.8, 3.7, 2.4) eV as the annealing time increases.

Keywords: Lead Oxide structure, DC sputtering, PbO roughness.

تأثير ازمنة التلدين على الخصائص التركيبية والبصرية لأغشية أوكسيد الرصاص المحضرة بتقنية الترذيذ بالتيار المستمر

اوس فيصل رؤوف* ، كاظم عبد الواحد عادم
قسم الفيزياء، كلية العلوم، جامعة بغداد، بغداد، العراق.

الخلاصة:
في هذا البحث تم ترسيب اغشية أوكسيد الرصاص باستخدام تقنية الترذيذ بالتيار المستمر على سطح ركيزة زجاجية وتم تلدينها حراريا عند درجة 473 كلفن ولثلاث فترات زمنية (ساعة واحدة وساعتان وثلاث ساعات). باستخدام تقنية (XRD) ومطياف القوى الذرية (AFM) وتقنية (FT-IR) وكذلك مطياف الامتصاص للأشعة المرئية وفوق البنفسجية (UV- Visible). كما تم تحديد الخصائص البصرية والتركيبية وتشكيلة السطوح للأغشية المحضرة والملدنة. ان الدراسات التركيبية اكدت التركيب متعدد السطوح للطور (Orthorhombic) لأغشية أوكسيد الرصاص بمعدلات حجم بلوري (24.51، 29.64، 46.49، 16.00) نانومتر كما وجد من فحص (AFM) ان خشونة السطوح (3.26، 1.76، 1.61، 1.79) نانو متر مع زيادة زمن التلدين وقيم فجوة الطاقة لأغشية أوكسيد الرصاص كانت (3.9، 2.8، 3.7، 2.4) الكتروفولت مع زيادة زمن التلدين.

*Email: aws.raouf1104@sc.uobaghdad.edu.iq

1. Introduction

Lead oxides find numerous applications in modern technology in different fields ranging from imaging devices to electrophotography and laser technology. On the other hand, PbO has been considered one of the interesting metal-oxide electrode materials for oxygen evolution reactions in applications such as fuel cells, hydrometallurgy, metal-air batteries, and solar-driven water splitting [1-3].

Therefore, several reports describe the properties and applications of lead oxides, including the electronic structure and bonding, the dielectric constant, electrophotography, oxygen gas sensing properties, and the photo conducting behavior of different lead oxides[4 -6]. Noticeable studies also denoted the characterization of PbO films produced by several methods, including chemical vapor deposition,[7] electrodeposition[8], Plasma magnetron sputtering[9], and reactive Rf sputtering [10]. However, to our knowledge, a few reports are available on the formation of PbO films produced by reactive DC sputtering. Reactive DC sputtering is an important industrial process for the deposition of metal–oxide films from elemental targets [11]. It has become the most widely used technique for the deposition metallic and compound thin films[12].

The present work reports a systematic investigation of the effect of annealing times on different PbO films by studying structural and optical properties. It is essential to understand the dependence of film properties upon different annealing times, as high-temperature applications of metal oxides have recently received considerable attention[13, 14]. At a varying annealing time, the optical and structural properties of the films may change, possibly also changing the film roughness, crystallite size, and relativity absorption. In addition, grain growth is possible for crystallite films, which could decrease surface roughness [15]. Furthermore, stoichiometric variations upon annealing are also possible. The efficiency and behavior of a material can be affected by its surface properties. It is possible to modify and tune these surface properties to meet a demand for improved performance [16]. Therefore, it is vital to determine and understand the annealing time dependence of film properties [17].

2. Experimental part

The experimental schematic setup of the DC sputtering system is shown in Figure (1). The system includes a vacuum chamber, made of glass, with a diameter of 29 cm and a height of 60 cm; this chamber contains a target (set as the cathode) and anode. The target was made of lead (supplied from Aldrich company with high purity (99.99) with diameters of 5 cm fixed at 2.5 cm from the anode. It was electrically connected to a variable high voltage DC power supply.

Lead oxide films were prepared by reactive D.C sputtering from a metallic lead target. Initially, the sputter chamber was pumped down to 8×10^{-2} mbar by a rotary vacuum pump. In our study, sputtering was performed at a pressure of 1×10^{-1} mbar, measured by an ion gauge, a constant cathode current of 40 mA, and a potential difference of 750 V. The lead target was sputtered by argon gas with a low rate of oxygen, where the oxygen partial pressure was controlled by regulating the oxygen flow rate. Thin films were deposited on glass substrates for 20 min. at 473K, the samples were annealed for different periods of (1, 2 and 3) hours in an oven (MEMMERT, made in Germany).

The structural investigations were done using XRD, AFM, and FT-IR techniques, which helped to determine the type of the morphplogy and microstructure of PbO. Thin films were examined by the XRD technique using a diffractometer (SHIMADZU made in Japan) of a power diffraction system with a Cu-Kα X-ray tube (λ=1.54060 Å, V=40kV, I=30mA, step 0.05, speed=5 deg/min). The X-ray diffraction was recorded with the diffraction angle 2θ in the range 14-45 degrees.

AFM (model TT-2), FT-IR (model spectrum TWO Perkin Elimer) with specteum rang (4000- 450) cm^{-1} and a double beam UV-Vis-NIR Metertech spectrophotometer(at varied (200–1100 nm) settings) were employed to study the prepared lead xide thin films.

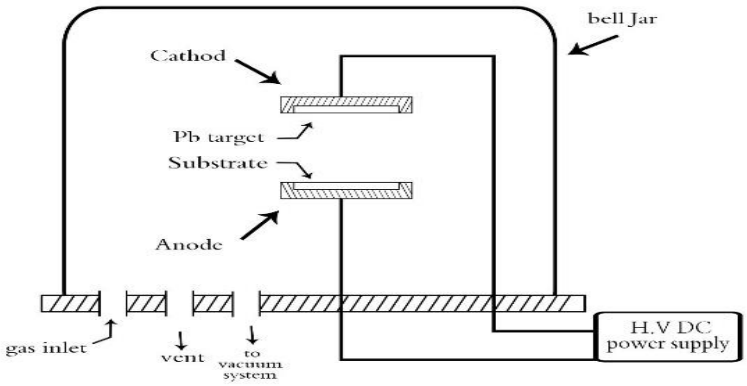

Figure 1: A sketch of a DC sputtering system.

3. Results

3.1. X-Ray Diffraction

Figure (2) illustrates the XRD patterns of PbO films for the as-deposited thin films and those annealed for three different annealing times. The diffraction pattern of PbO matched with that of the International Centre for Diffraction Data (ICDD) card number [98-900-7711], confirming the type of film to be PbO and has an orthorhombic crystal system [18]. The Crystallites size has been estimated using Scherrer's relation [19]:

$$D = \frac{k\lambda}{\beta cos\theta} \quad (1)$$

Where: D is the Crystallites size, k is a constant that depends on the relative orientation of the scattering vector to the external shape of the crystallite[20], λ is the wavelength, β is the width of the XRD line, and θ is diffracting angle from the Bragg's angle position. Upon annealing the pristine PbO films at 473K for 1, 2, and 3 hours, it becomes a polycrystalline's structure. The XRD pattern for annealed PbO film confirms the presence of the PbO phase within the orthorhombic crystal system. This result is similar to the findings of Zeyada and Makhlouf [21] and Alagar et al. [22]. It can be observed from the figure that the pristine film has seven distinct peaks at (2θ =20.2º,21.24º,24.9º, 27.4º,29.3º, 30.6º, 34.4º) with the orientations (020, 110,110 111, 111 200, 002), respectively. After 1 hour of annealing, five peaks disappeared while the peaks at (2θ= 29.3º and 30.6º) became more intense, and new peaks appeared at (2θ= 32.9º,38.1º) with orientations (111, 200), respectively. These additional peaks which appeared in the one-hour annealed sample corresponding to Pb_3O_4 are identical with standard card No. 96-901- 2703. This is similar to the findings of Hamid and Mohammed [23]. The samples annealed for 2 hours showed many peaks located at 2θ = 15.3,20.2º,21.24º,24.9º, 27.4º,29.3º, 30.6º, 32.9, and 38.1º). The intensity of the most pronounced peaks at 2θ= 29.3º and 30.6º became sharper indicating additional crystal growth along these planes giving rise to large crystallite size, as shown in Table (1). After 3 hours of annealing, most of the peaks vanished; the peaks at (29.3º, 30.6º) became wider with a shoulder around the peak (2θ=30º). It is clearly observed that there was an inverse relationship between peak intensity, crystallite

size, and the FWHM. There was a slow growth rate of particle sizes at higher annealing times, whose growth speed was low compared to that at intermediate annealing times.

The retardation of crystal growth was attributed to the time of annealing, which worsened the crystalline structure due to the energy supplied to the atoms that hindered the gathering of atoms and hence reduced the particle size of the lead oxide thin films [24].

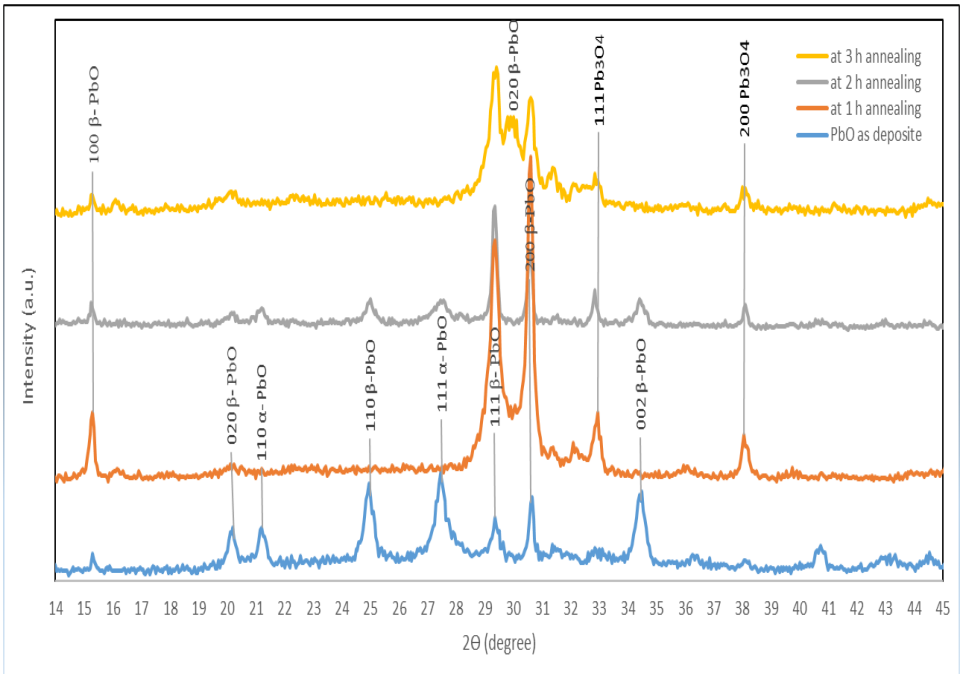

Figure 2: XRD patterns of PbO thin films annealed at 473k for different period times.

The crystallite sizes at the most intense peaks were calculated and listed in Table (1). It was well pronounced that the average crystal size reached a maximum of (46.49) nm after a thermal annealing time of 2 hours. This indicated that increasing thermal annealing time first enhanced the crystal structure, but then the opposite took place.

Table 1: the variation of crystal sizes at different annealing times.

2θ	crystal size (nm)			
	as deposit	**1 hour**	**2 hours**	**3 hours**
29.3°	22.56	23.55	46.00	14.64
30.6°	26.38	35.73	46.98	17.37
Average	**24.51**	**29.64**	**46.49**	**16.00**

3.2. Atomic Force Microscopy (AFM).

The surface topography of the formed thin films was studied using AFM analysis, which analyzes the surface of the samples, produces microscopic images of their state and gives statistical values of several variables. The average roughness and root mean square (RMS) were deduced from the AFM images. Figure (3) shows 3D AFM images for lead oxide thin films annealed at a temperature of 473K for different times. A sponge-like structure appeared, and the thin film covered all the surfaces of the glass substrate.

The finer morphology and roughness of the films can be seen for (PbO) thin films. The roughness of the surface is an important parameter which describes the scattering of light and gives an idea about the quality of the surface under investigation. In addition, it provides some

insight into the growth morphology. The decrease in surface roughness of the annealed films leads to a reduction in the efficiency of sensing properties. Therefore, it is vital to investigate the surface morphology of the films. Table (2) shows the results of AFM analysis for (PbO) for the three annealing times. It can be noted that the average roughness decreased from 3.26 nm to 1.79 nm as the annealing time increased because the shrinking lattices led to a reduction in the grain size.

Table 2: The results of AFM analysis for (PbO) at 3 time periods of annealing at 473k.

Sample	Average Roughness	R.M.S
PbO as deposit	3.26 nm	4.88 nm
PbO at 1 hour	1.76 nm	2.37 nm
PbO at 2 hour	1.61nm	2.19 nm
PbO at 3 hour	1.79 nm	2.52 nm

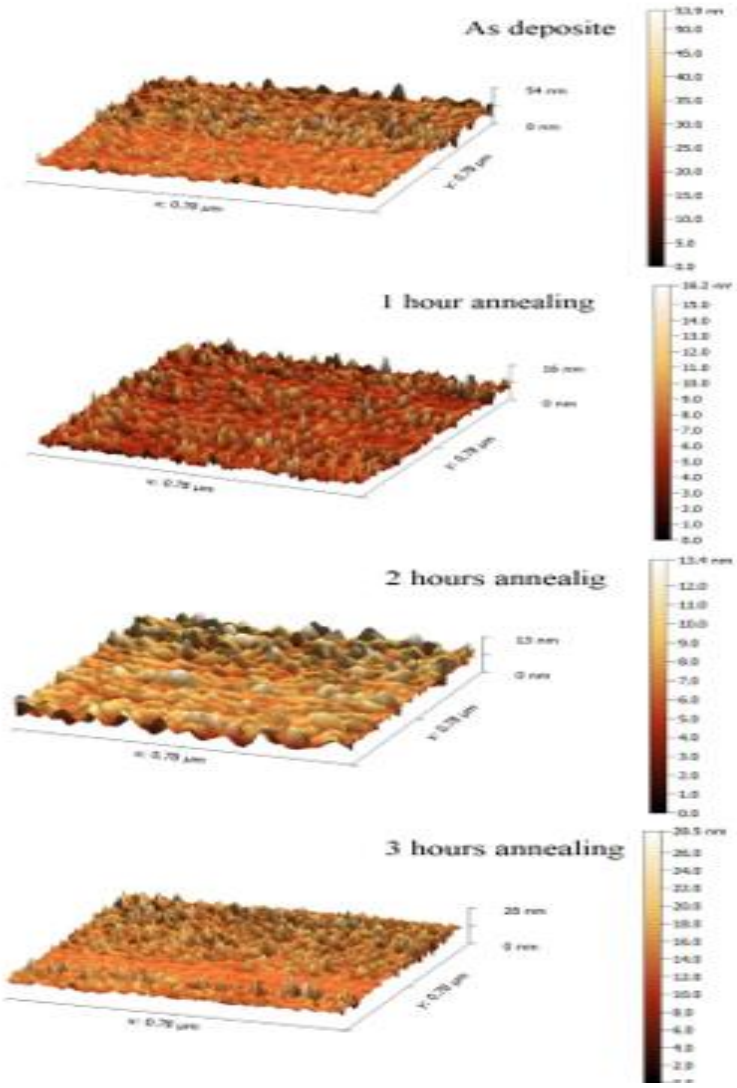

Figure 3: AFM image at 473k for pristine for the three annealing times.

Both average roughness and RMS values decreased after annealing compared to their values without annealing. This is because annealing increases the collisions between molecules and thus has the lowest kinetic energy. Figure (3) shows the results of the granularity distribution

of average diameter obtained from the AFM analysis of the PbO thin films. The value of grain size distribution of the films was clear at room temperature (RT) and annealing temperature.

3.3. Fourier-transform infrared spectroscopy (FT-IR)

FT-IR spectrum for the lead oxide is shown in Figure (4). This spectrum has different transmission peaks. A strong peak at 1393 cm^{-1} corresponds to the Pb-O stretching, and another peak at 682.9 cm^{-1} indicates the presence of lead [25]. The transmission peak at 460 cm^{-1} indicates the presence of (Pb-O) stretching vibration mode [26,27]. The peak around 833 cm^{-1} is due to the Pb-O vibrations, and the peak around 700 cm^{-1} is related to the asymmetric bending vibration of Pb-O-Pb [28][29]. The peaks located at 3735 cm^{-1} correspond to the bonding of H–OH stretching bonding modes of water[30], while the infrared peaks located at (2923, 2853, 1743) cm^{-1} and 1650 cm^{-1} are related to the (C=O) stretching vibration modes that refer to the little contribution of CO_2 dissolution from air contain [31].

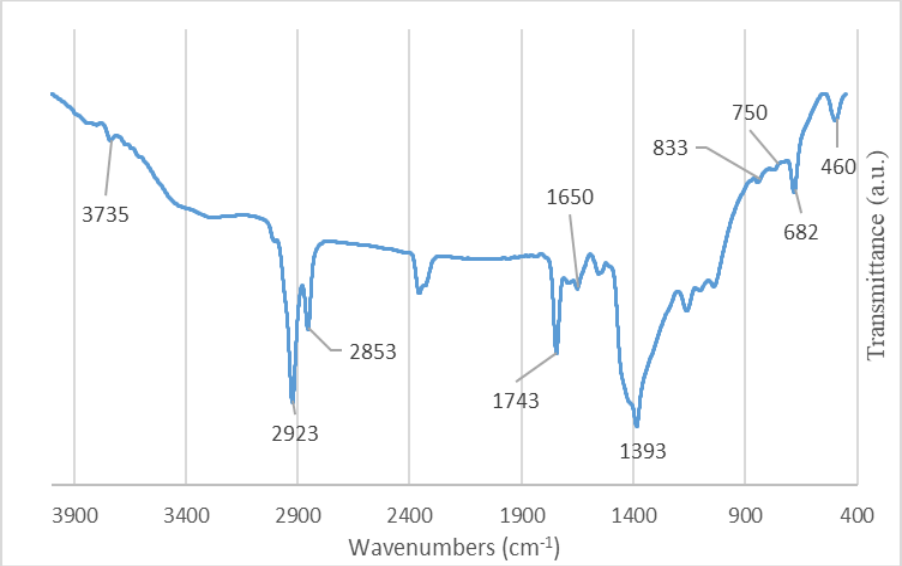

Figure 4: FT-IR spectrum of lead oxide

3.4. UV-VIS properties

The absorbance spectra of the as-deposited lead oxide thin film and those annealed at 473K for different times (1,2 and 3 hours) are revealed in Figure (5). It is obvious that the absorption edge shifted to a longer wavelength (redshift) due to the annealing of the as-deposited lead oxide thin films for one hour; this was followed by a blue shift, i.e., shift to the short wavelength side as a result of increasing the annealing time of the deposited thin films to 2 hours; eventually the absorption edge return to shift to longer wavelength (red shift) as a result of increasing the annealing time to 3 hours. This irregular shift of the absorption edge was reflected in the energy gap values, as seen in the next section.

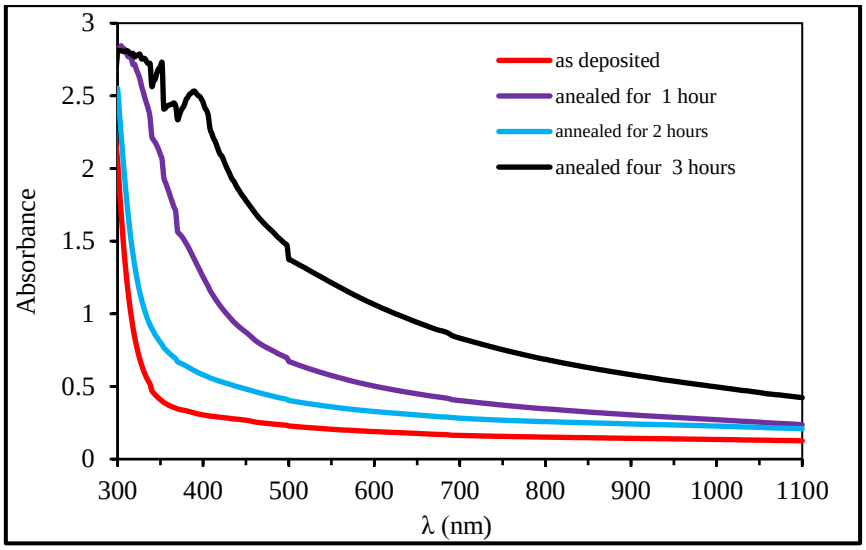

Figure 5: The absorbance spectra of lead oxide thin films annealed at 473K at different annealing times

The optical band gap was graphically found using Tauc's formula [32][33] for direct transition:

$$(\alpha h\upsilon)^2 = A\,(h\upsilon - Eg) \quad (2)$$

Where: Eg is the optical energy gap, α is the absorption coefficient, hυ is the photon energy of incident light, and A is a constant. The graphs in Figure (6) reveal that the pristine films have a direct allowed energy gap of 3.9eV, which decreased after annealing for 1 hour to 2.8 eV; this can be attributed to the increase of the particle size, as demonstrated in the XRD results. After annealing for 2 hours, the energy gap was found to increase to 3.7 eV. Finally, the energy gap was drastically reduced to 2.4 eV after thermal treatment for 3 hours. This can be attributed to creating new localized states by the effect of the long period of thermal treatment, which permits re-arranging the deposited atoms. Table 3 illustrates the bandgap energies at the different thermal treatment times. The shifts of energy gap toward longer wavelengths (low energies) with the increase of thermal annealing time are related to the growth of grain size; the growth of grain size reduces the lattice parameters and hence reduces the energy gap.

The calculated values of band gap energy for β-PbO are much higher than that of bulk PbO, which in fact, clearly indicates that the synthesized products are in the nanoscale. Further, a relatively higher value of the energy of smaller size β-PbO agrees well with the concept that band gap increases with decreasing particle size [34, 35].

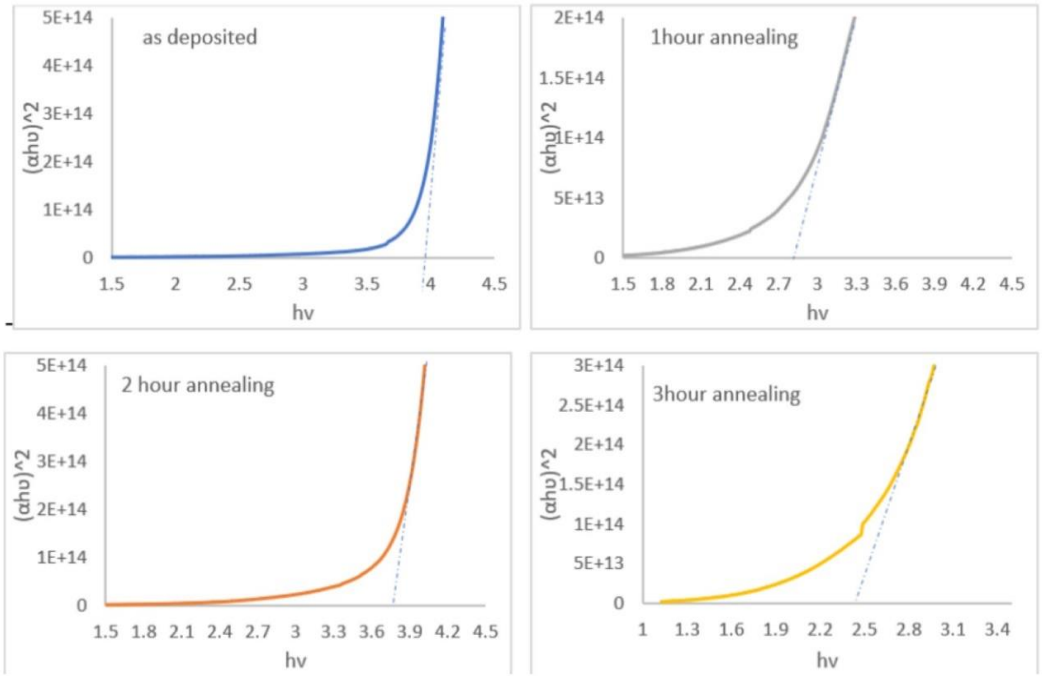

Figure 6: the relation between $(\alpha h\nu)^2$ and hν of PbO at different annealing times at 473k.

To investigate the effect of thermal treatment time on the localized states in extremities of the valence and the conduction band the Urbach Rule was used. The absorption edge becomes wide for polycrystalline and amorphous semiconductors because allowed localized states are found in the energy gap. The width of these localized states can be calculated using Urbach Rule[36]

$$\alpha = \alpha_0 e^{h\nu/E_u} \quad (3)$$

Where: (α_0) is constant, and E_u is the width of localized states. The plot of ln (α) and energy was drawn as shown in Figure (7). The width values on localized states are determined and listed in Table (3). Thus the drastic reduction of energy gap value can be explained based on the high energy of thermal treatment, which introduce energy levels in the forbidden gap which causes radical changes in the carries concentration; these new levels may be acceptors at the top of the VB or donor levels below the CB Thus; definitely, the energy required to transport the charge carrier between these levels will be lower than that required to transport the charge carrier from the VB to the CB [37].

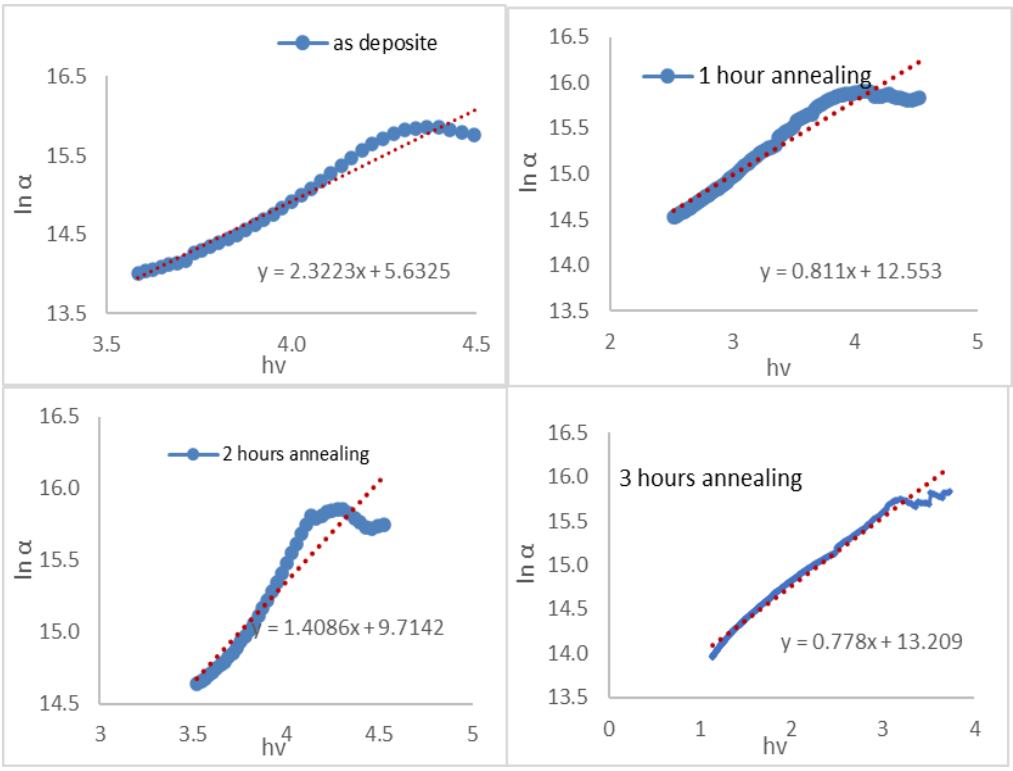

Figure 7 : the relation between ln(α) and (hν).

Along the absorption curve and near the optical band edge, there is an exponential part called the Urbach tail, and the energy of this part is known as Urbach tail energy. Urbach tail energy represents the measure of structural disorder in the thin film network. The effect of annealing time into the semiconducting PbO thin film reveals the formation of band tailing in the band gap called Urbach tail are predicted obeying the Urbach rule in the low photon energy range: Eu is the Urbach energy, which characterizes the slope of the exponential edge and measures the disorder in the structure of the material. By plotting ln(α) against the incident photon energy (hν) , Figure (6), the band tail energy, i.e., Urbach energy (Eu), was determined from the reciprocal slope of the linear portion. The findings indicated that the Urbach energy of PbO thin films increased by annealing the thin films due to the smaller density of localized states. Table (3) reveals that the Urbach energy (Eu) increased from 0.43 eV to 1.28 eV, and optical band gap energy (Eg) decreased from 3.9 eV to 2.8 eV for the one hour annealed thin films. These findings indicated an increase in structural disorder and defects in PbO thin films[38]. It is obvious that the depth of tail states changes in the opposite manner to that of the energy gap; thus, the maximum value of the tail state (1.28 eV) corresponded to the narrower band gap (2.4 eV) and verse versa.

The localized states are more pronounced for the high annealing time; also, the crystal structure exhibited a low degree of crystallinity (as shown from XRD). It is well known that the depth of localized state values increases with increasing absorbance, i.e., the maximum value of (Eu) corresponding to the minimum energy gap value, which is related to the defect states introduced by the thermal annealing, as seen in Table (3).

Table 3: The band gap energies and the width of localized states at different annealing times.

Annealing time	Energy gap	Eu (eV)
As deposited	3.9 eV	0.43
1 hour annealing	2.8 eV	1.19
2 hour annealing	3.7 eV	1.23
3 hour annealing	2.4 eV	1.28

4. Conclusion.

In this research, the structural and optical behavior of PbO films prepared by DC sputtering was studied. The structural studies confirmed that lead oxide films are polycrystalline's structures in an orthorhombic phase. It was found that increasing thermal treatment time enhanced the crystal structure first, but then the opposite took place; the roughness of the film surface decreased as the film annealing time increased. The optical band gap values of the lead oxide thin films were found to change in a non-regular manner as the annealing time increased.

References

[1] M. Batool, R. Gill, K. Munawar, V. McKee, and M. Mazhar, " Single source precursor derived ZnO–PbO composite thin films for enhanced photocatalytic activity," *Journal of Solid State Chemistry,* vol. 305, no 122642, pp 1-9, 2022.

[2] M. Nadeem, Y. Li, H. J. M. Bouwmeester, and C. Xia, " PbO effect on the oxygen reduction reaction in intermediate-temperature solid oxide fuel cell," *International Journal of Hydrogen Energy*, vol. 45, no. 46, pp 25299-25306, 2020.

[3] A. Calisan, C. G. Ogulgonen, S. Kincal, and D. Uner, "Finding the optimum between volatility and cycle temperatures in solar thermochemical hydrogen production: Pb/PbO pair," *International Journal of Hydrogen Energy*, vol. 44, no. 34, pp 18671-18681, 2019.

[4] S. H. Elazoumi et al., "Effect of PbO on optical properties of tellurite glass," *Results in Physics,* vol. 8, no 1, pp 16-25, 2018.

[5] A. Bakhtatou and F. Ersan, "Effects of the number of layers on the vibrational, electronic and optical properties of alpha lead oxide," *Physical Chemistry Chemical Physics*, vol. 21, no. 7, pp 3868-3876 ,2019.

[6] D.D.O. Eya, "Influence of Thermal Annealing on the Structural and Optical Properties of Lead Oxide Thin Films Prepared by Chemical Bath Deposition Technique," *The Pacific Journal of Science and Technology,* vol. 7, no 2, pp. 114–119, 2006.

[7] W. Steckelmacher, "Handbook of thin film process technology," *Vacuum*, vol. 47, no. 3, 1996.

[8] Y. Yao, C. Huang, H. Dong, F. Wei, and X. Chen, "Influence of Manganese Ions on the Electrodeposition Process of Lead Dioxide in Lead Nitrate Solution," *Russian Journal of Electrochemistry,* vol. 55, no. 5, pp 364-369 ,2019.

[9] K. A. Yahya, "Effect of electrode separation in magnetron DC plasma sputtering on grain size of gold coated samples," *Iraqi Journal of Physics (IJP),* vol. 15, no. 35,pp 202-210, 2017.

[10] V. D. del Cacho, L. R. Kassab, A. D. dos Santos, A. L. Siarkowski, D. M. da Silva, and N. I. Morimoto, " Fabrication and Characterization of GeO_2 -PbO Optical Waveguides," *ECS Transactions,* vol. 23, no. 1, pp 1-23, 2009.

[11] S. Venkataraj, J. Geurts, H. Weis, O. Kappertz, W. Njoroge, R. Jayavel, and M. Wuttig, " Structural and optical properties of thin lead oxide films produced by reactive direct current magnetron sputtering," *Journal of Vacuum Science & Technology A: Vacuum, Surfaces, and Films,* vol. 19, no. 6, pp 2870-2878, 2001.

[12] J. T. Gudmundsson, "Physics and technology of magnetron sputtering discharges," *Plasma Sources Science and Technology*, vol. 29, no. 11, pp 2870-2878, 2001.

[13] Q. Kang, F. Yang, X. Zhang, and Z. Hu, "Mechanical and optical behaviors: strain synergy effects in high temperature phase oxides of lead," *New Journal of Chemistry*, vol. 45, no. 42, pp 19714-19722 , 2021.

[14] Y. X. Zheng, J. F. Lv, H. Wang, S. M. Wen, and L. Huang, "Efficient sulfidization of lead oxide at high temperature using pyrite as vulcanizing reagent," *Physicochemical Problems of Mineral Processing*, vol. 54, no. 2, pp 270-277, 2018.

[15] A. A. P. Frit, K. Deepalakshmi, N. Prithivikumaran, and N. Jeyakumaran", The effect of annealing time on lead oxide thin films coated on indium tin oxide substrate," *International Journal of ChemTech Research*, vol. 6, no. 13, pp 5347-5352 , 2014.

[16] Moatasim Amer, "Effect of FilmsThickness on Structural and Optical Properties of Gold (Au) Thin Films Prepared by DC Magnetron Sputtering," *Iraqi Journal of Science*, vol. 63, no. 4, pp. 1549–1556, 2022.

[17] S. Venkataraj, O. Kappertz, R. Drese, C. Liesch, R. Jayavel, and M. Wuttig, " Thermal stability of lead oxide films prepared by reactive DC magnetron sputtering," *Physica Status Solidi (A) Applied Research*, vol. 194, no. 1, pp 192-205, 2002.

[18] S. N. Kabekkodu, J. Faber, and T. Fawcett, " New Powder Diffraction File (PDF-4) in relational database format: Advantages and data-mining capabilities," *Acta Crystallographica Section B: Structural Science*, vol. 58, no. 3, pp 333-337, 2002.

[19] J. Zhou and H. Wang, " The physical meanings of 5 basic parameters for an X-ray diffraction peak and their application," *Chinese Journal of Geochemistry*, vol. 22, no. 1, pp 38-44, 2003.

[20] M. A. R. Miranda and J. M. Sasaki, "The limit of application of the Scherrer equation," *Acta Crystallographica Section A: Foundations and Advances*, vol. 74, no. 1, pp 54-65, 2018.

[21] H. M. Zeyada and M. M. Makhlouf, "Role of annealing temperatures on structure polymorphism, linear and nonlinear optical properties of nanostructure lead dioxide thin films," *Opt Mater (Amst)*, vol. 54, no 1, pp 181-189, 2016.

[22] M. Alagar, T. Theivasanthi, and A. Kubera Raja, " Chemical synthesis of nano-sized particles of lead oxide and their characterization studies," *Journal of Applied Sciences*, vol. 12, no. 4, pp 1-8 , 2012.

[23] R. Hamid and Maad Mohammed, " Effect of Annealing on the structural, surface morphology and optical properties for CdO: PbO composite thin films," *Al-Qadisiyah Journal Of Pure Science*, vol. 26, no. 3, pp 1-9 , 2021.

[24] A. M. Luís, M. C. Neves, M. H. Mendonça, and O. C. Monteiro, "Influence of calcination parameters on the TiO_2 photocatalytic properties," *Materials Chemistry and Physics*, vol. 125, no.1, pp 20-25, 2011.

[25] A. Güngör, R. Genç, and T. Özdemir, " Facile synthesis of semiconducting nano-sized 0d and 2d lead oxides using a modified co-precipitation method," *Journal of the Turkish Chemical Society, Section A: Chemistry*, vol. 4m, no. 3, pp 1017-1030, 2017.

[26] D. K. M. Al-Nasrawy, " Microstructure properties of lead silicate glasses," Iraqi Journal *of Physics (IJP)*, vol. 13, no. 28, pp 91-99, 2019.

[27] H. H. Rashed, F. A. Fadhil, and I. H. Hadi, " Preparation and characterization of lead oxide nanoparticles by laser ablation as antibacterial agent," *Baghdad Science Journal*, vol. 14, no. 4, pp 801-807, 2017.

[28] Y. Azizian-Kalandaragh, " Preparation of lead oxide nanostructures in presence of polyvinyl alcohol (PVA) as capping agent and investigation of their structural and optical properties," *Journal of Semiconductor Technology and Science*, vol. 18, no. 1, pp 91-99, 2018.

[29] J. Senvaitiene, J. Smirnova, A. Beganskiene, and A. Kareiva, " XRD and FTIR characterisation of lead oxide-based pigments and glazes, " *Acta Chimica Slovenica*, vol. 54, no. 1, pp 185–193 ,2007.

[30] A. A. Ramadhan, " Effect of annealing and chemical treatment on structural and optical properties of CuPcTs/PEDOT:PSS (BHJ Blend) thin films," *Iraqi Journal of Physics (IJP*), vol. 15, no. 33, pp 131-142 , 2019.

[31] A. B. D. Nandiyanto, R. Oktiani, and R. Ragadhita, " How to read and interpret ftir spectroscope of organic material," *Indonesian Journal of Science and Technology*, vol. 4, no. 1, pp 97-118, 2019.

[32] M. A. Fakhri, Y. Al-Douri, U. Hashim, and E. T. Salim, " Optical investigations of photonics lithium niobate," *Solar Energy*, vol. 120, no 1, pp 381-388, 2015.

[33] G. H. Jihad, "Synthesis and Characterization of α-Fe2O3 Nanoparticles Prepared by PLD at Different Laser Energies," *Iraqi Journal of Science*, vol. 62, no. 11,pp 3901-3910, 2021.

[34] K. T. Arulmozhi and N. Mythili, " Studies on the chemical synthesis and characterization of lead oxide nanoparticles with different organic capping agents," *AIP Advances*, vol. 3, no. 12, pp 1-9, 2013.

[35] N. Mythili and K.T. Arulmozhi, " Characterization studies on the chemically synthesized α and β phase PbO nanoparticles," *International Journal of Scientific & Engineering Research*, vol. 5, no. 1, pp. 412–416, 2014.

[36] M. Bhowmick, H. Xiz, and B. Ullrich, " Optical bandgap definition via a modified form of Urbach's rule," *Materials*, vol. 14, no. 7, pp 1-6, 2021.

[37] J. Shirafuji, G. il Kim, and Y. Inuishi, "Photoluminescence and optical properties of $Ge_{1-x}Se_x$ glasses," *Japanese Journal of Applied Physics*, vol. 16, no. 1,pp 67-76, 1977.

[38] H. Yamamoto, S. Tanaka, and K. Hirao, "Effects of substrate temperature on nanostructure and band structure of sputtered Co3O4 thin films," *Journal of Applied Physics*, vol. 93, no. 7, pp 4158-4162, 2003.